Proceedings of the XVII ECSMGE-2019
Geotechnical Engineering foundation of the future
ISBN 978-9935-9436-1-3

doi: 10.32075/17ECSMGE-2019-0169

XVII European Conference
ECSMGE 2019
Reykjavik
on Soil Mechanics
and Geotechnical Engineering

Full-scale tests and three-dimensional finite element analysis on micropile groups

Essais à grande échelle et analyse éléments finis en 3D de groupes de micropieux

M. Allani
Belgian Building Research Institute (BBRI), Geotechnics Division, Limelette, Belgium

N. Huybrechts
Belgian Building Research Institute (BBRI), Geotechnics Division, Limelette, Belgium
KU Leuven, Department of Civil Engineering, Leuven, Belgium

ABSTRACT: In order to study in detail the effect of micropile group behaviour in terms of group efficiency (ULS) and settlement (SLS), a real-scale test campaign on micropiles has been set up on the Limelette test field of the Belgian Building Research Institute (BBRI). This paper reports the results of axial static load tests of two single micropiles and two micropile groups existing out of 5 and 9 micropiles respectively. All the tested micropiles have a diameter of 150 mm and are installed at a depth of 6 m in a silty layer. To capture the load transfer curves, all the micropiles were instrumented over their entire length with Fibre Bragg Grating (FBG) optical sensors. A 3D finite element model (FEM) was then build and fitted to the measurements for the single micropiles. Good matching was then obtained for the settlement of micropile groups.

RÉSUMÉ: Dans le but d'étudier en détail l'effet de groupe de micropieux et ce en termes de capacité portante (ELU) et de tassement (ELS), une campagne d'essais à grande échelle a été menée sur le site expérimental de Limelette au sein du Centre Scientifique et Technique de la construction (CSTC). Cet article résume l'ensemble d'essais de mise en charge statique réalisés sur deux micropieux isolés et sur deux groupes de micropieux: le premier groupe est constitué de cinq micropieux et le deuxième de 9 micropieux. Tous les micropieux, d'un diamètre de 150 mm, ont été installés à 6 m de profondeur dans une couche de limon. Afin de déduire les courbes de transfert, les micropieux ont été équipés sur toute la longueur de capteurs à fibre optique Fibre Bragg Grating (FBG). Un modèle éléments finis a été calé sur les mesures des micropieux isolés. Une bonne correspondance a été retrouvée pour le tassement des groupes.

Keywords: micropile; group effect; full-scale tests; 3D finite element analysis;

1 INTRODUCTION

Several approaches can be used to assess the settlement of single piles and pile groups: the boundary element methods (Poulos 1968; Butterfield and Banerjee 1971), the finite element method (McCabe and Lehane, 2006) or approximate solutions such as load transfer approach (Randolph & Wroth, 1978; Fleming, 1992; Mylonakis and Gazetas, 1998). Despite these theoretical advances in the analysis and prediction of pile group behaviour in the last few decades, these methods are still based on simplifications of the problem and of the constitutive behaviour of the soil. Consequently, static load tests on pile groups remain the most reliable means of assessing pile group response. Micropiles are small diameter drilled and grouted piles (less than 300 mm). The execution principles are described in EN 14199. Juran et al, 1999 presented an excellent state of the art covering all studies and contribution for micropile practice. Despite the widespread use of micropiles, field tests results on micropile groups are limited in the literature. This paper provide experimental results on micropile groups during a well instrumented real-scale test campaign. Behaviour of the micropile groups is then fitted through a calibrated 3D finite element model.

2 EXPERIMENTAL PROGRAM

The BBRI organised during (2012-2014 and 2014-2016), with the financial support of the Federal Public Service Economy and the Belgian Bureau for Standardisation (NBN) a research project on micropiles. The first plan (2012-2014) was focussed on ultimate load design of single micropiles. The second plan (2014-2016) was focussed on the group and cyclic effects of micropiles. Only the group effects are considered in this paper.

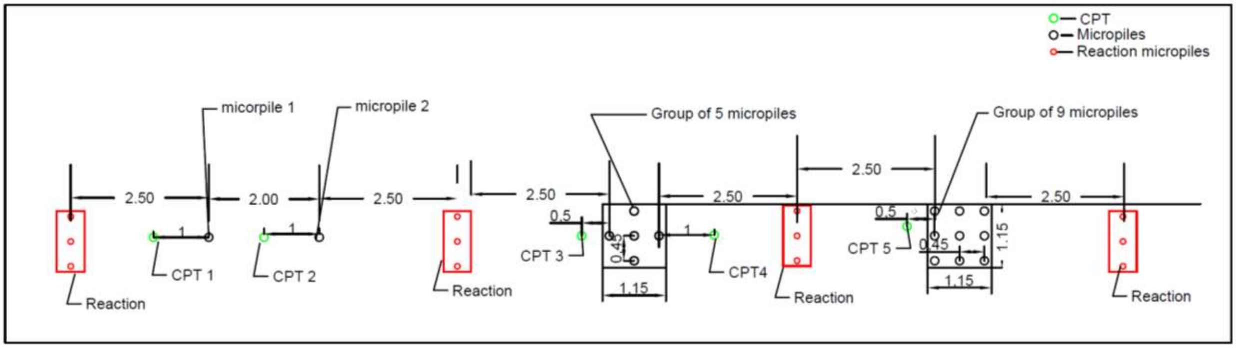

Figure 1. Micropile configuration (quotations in m)

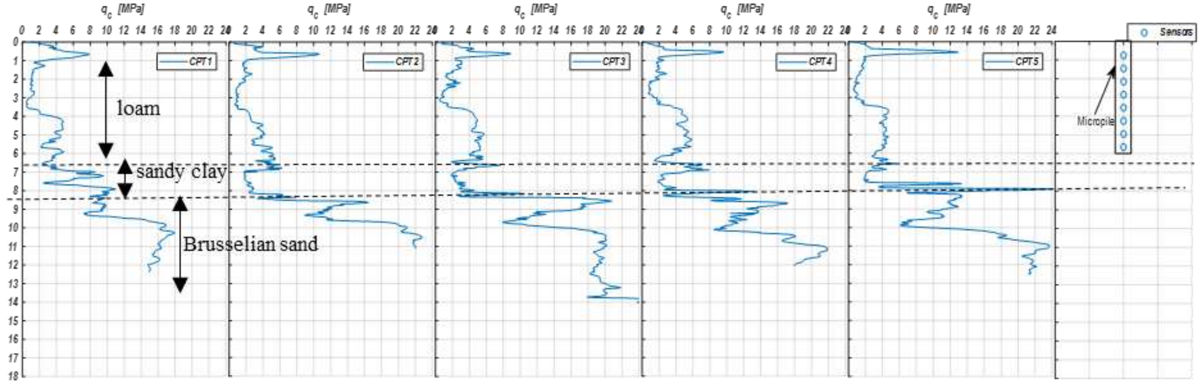

Figure 2. CPTs profiles and sensors position

2.1 Micropile configurations

A full-scale test campaign involving two isolated micropiles M1 and M2; and two micropile groups was conducted. The first group G5 is composed of five micropiles and the second group G9 is composed of nine micropiles (Figure. 1).

All micropiles were realized with self-drilling hollow rods (TITAN 52/26) at the end provided with a sacrificial drill bit. The diameter of the bit is 150 mm and represents the nominal diameter of the micropiles. The micropiles are installed at a depth of 6 m in the loam layer. The distance between micropiles in groups G5 and G9 is equal to 3 times the nominal diameter.

2.2 Site characterization

The test site is located at the Belgium Building Research Institute (BBRI) in Limelette (Belgium). The geotechnical soil parameters for the Limelette site are well documented in the work of Van Alboom and Whenham (2003). The site of Limelette is characterised by quaternary loam overlaying a tertiary sand (Brusselian sand). Five CPTs were performed nearby the installed micropiles. According to CPT tests (Figure. 2), it was concluded that the soil profile consists out of silt (loam) from 2.2 to 6.2 m, sandy clay from 6.2 to 8.2 m and slightly clayey sand (Brusselian sand) from 8.2 to 17m. The groundwater level is very deep.

2.3 Micropile installation

Self-drilling rods of the type R51N (TITAN 52/26) (Figure. 3a.), manufactured by the company Ischebeck, with a drill bit diameter of 150 mm are installed. This type of bit (R51CRC150) is specifically used for cohesive soils (Figure. 3b). The drilling procedure was performed with water injection through the hollow rods and the drill bit with a rotation speed of about 152T/min. The hollow bars were supplied in 3 m sections and coupled together with 160 mm long coupling sleeve (Figure 3). After reaching a depth of 6 m the spoil is replaced by a grout injection with a water/cement ratio of W/C=0.6. The total volume needed per micropile was around 140 l. No post-injection was carried out. This procedure can be considered as a grouting gravity process.

2.4 Micropile instrumentation

The load on the micropiles is applied with one (single micropiles) or two (micropile groups) hydraulic jacks of 2 000 kN each. The hydraulic jacks are regulated by a high precision hydraulic unit (PLC regulation) to ensure a constant load at each loading step.


a) b)

Figure 3. a) Self-boring bars and b) drill bit

The applied load at the pile head is measured by calibrated load cells. The head displacement of each micropile is measured with electronic displacement sensors (resolution 0.01 mm) (Figure 4). The displacement of the micropiles head is also verified by a total station. To determine the load distribution during the test, strains are measured at different levels (Figure. 2) in the micropiles using optical fibre sensors FBGs type. These sensors have been installed by grout connection in the existing hollow bars of the micropiles (Figure 4). Strains are given in microstrain ($1\ \mu S = 10^{-6}$ m/m). The strains are analysed using the Fellenius (2001) method to determine the modulus of elasticity and to derive forces from strains. All micropiles (single and in group) were equipped with optical fibres FBGs (Figure. 5). The position of the sensors are given in Figure 2.

2.5 Test procedure

A reaction system was designed to perform the micropile load tests. The reaction frame involved a loading steel plate (1150 mm*1150 mm*150 mm), two steel reaction beams (HEB 800 with 8 m length), 3 self-drilling reaction micropiles on each side (9 in total) with a nominal diameter of 150 mm installed at a depth of 12 m. The 150 mm

thick steel plate served as a pile cap for the micropile groups (Figure 4) and elevated to avoid contact with the soil (avoiding a pile-raft system). It is connected through spherical hex nuts (at the top and at the bottom) to micropiles. No loading plate was used for the isolated micropiles. However, a special cylinder lock strap was manufactured as shown in Figure 6. As recommended by the ISSMFE (1980), reaction micropiles are located at 2.5 m away from the extremity of tested micropiles. This eliminates a possible interaction between the tested micropiles and reaction micropiles. The reaction system is configured to serve for compression tests as well as tension tests. An Overview of the reaction system is given in Figure 7. A Series of cyclic and static tests were programed for the test campaign. Cyclic behaviour is out of the scope of this paper and only the first static load tests are considered.
To avoid bringing up the micropiles to failure before applying the cyclic loads, the first static tests are conducted until the creep load which is by convention determined as the load corresponding with a creep rate of $\alpha = 1$ mm. α per each load step is determined as:

$$\alpha = \frac{s_{\mathrm{t=60min}} - s_{\mathrm{t=30min}}}{log10\,(2)} \qquad (1)$$

Where s_{t} is the micropile head settlement at time t for each load step.

The applied static loading procedure is based on the ISSMFE (1985) procedure and conforms to the Belgian practice.

Figure 4. Micropile group instrumentation

3 ANALYSIS OF LOAD TEST RESULTS

3.1 Single micropile test results

The load-settlement curve of the single micropiles is given in Figure 8. Both tests were stopped at a load corresponding to a creep rate $\alpha \approx 1$. The evolution of the creep rate in function of the applied load is given in Figure 9. The creep load for single micropiles corresponds to a load of 180 kN. Both single micropiles showed a similar behaviour which reflects the homogeneity/repeatability of the results. Figures 10 shows the axial force versus depth along the micropiles. These are derived from the strains measurement using the Fellinus (2001) approach. There is a significant transfer of load between 2.5 and 6 m showing that the micropile resistance is mainly composed by the shaft resistance (base resistance represents only 18% and 7% of the total resistance for micropile 1 and 2, respectively).

Figure 5. Optical fiber sensors installation

Figure 6. Singular micropile instrumentation

Figure 7. Overview of the reaction system (9 micropiles group)

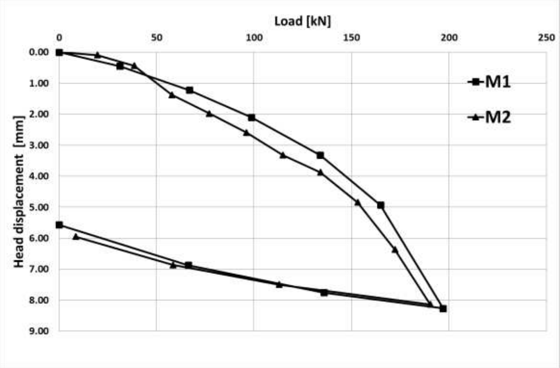

Figure 8. Load-settlement curve for single micropiles

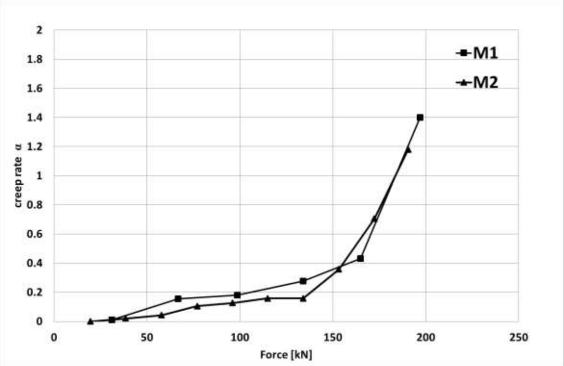

Figure 9. Creep rate in function of the load

3.2 Pile group results

Figure 11 shows the load-settlement curves for single micropiles and the average (per micropile) load-settlement curves for the micropile groups. The settlement of the individual micropiles in the groups are measured separately and the average value is considered. It is observed that G9 showed a stiffer behaviour in first loading steps. However, from a certain average load per micropile in the group (round. 120 kN), the group settlement is larger than the settlement of the single micropiles under that same average load. This is confirmed by the evolution of the creep rate as a function of the load for single micropiles and as a function of the average load per micropile in the groups (Figure 12). The creep load per micropile is equal to 150 and 130 kN for the group G5 and G9, respectively. These values are smaller than those for single micropile (180 kN). Verification of pile group design either in ultimate limit state or in serviceability limit state is in reality a settlement verification. In fact, the ultimate load could be defined (EC7) as the load that causes a settlement of 10% of the pile diameter. Since tests are stopped at the creep load, a hyperbolic fitting (Fleming, 1992) of the load-displacement is adopted to derive the ultimate load (considered at 15 mm of displacement). For M1 and M2 the ultimate load is estimated at 233 and 243 kN, respectively. An average load per micropile of 183 and 161 kN is found for G5 and G9, respectively. As the evaluation of settlement is primary for pile group design, the group settlement ratio R_s is often used. It is defined as the ratio of the settlement of the pile group divided to that of single pile at the same average load.

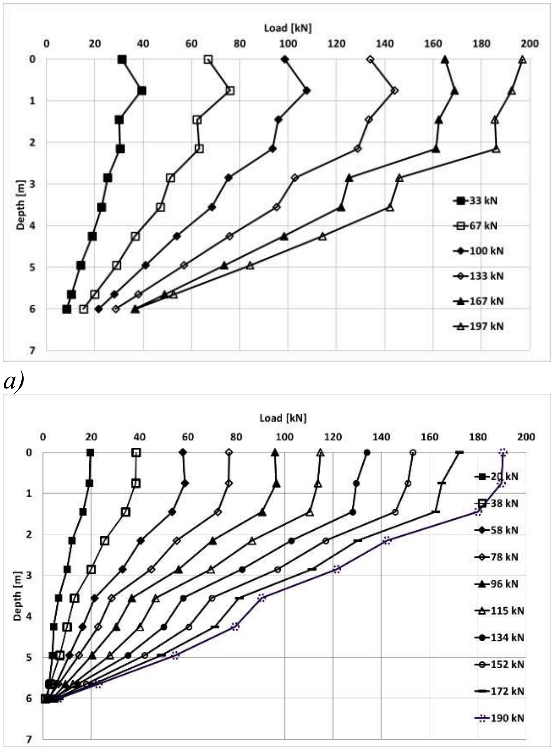

a)

b)

Figure 10. Axial force distribution along the micropile depth as function of load steps a) M1 and b) M2

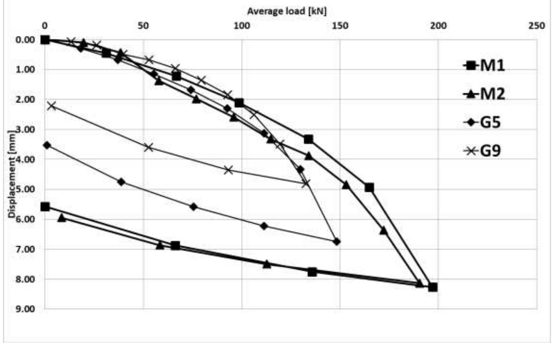

Figure 11. Comparison between load-settlement curves for single micropiles and micropile groups

Figure 13 shows the value of R_s as a function of the group settlement based on the hyperbolic fitting. The value of R_s tends to increase with the group settlement. The single pile settlement is generally smaller than the corresponding pile group settlement at average load ($Rs > 1$) especially when the load is large.

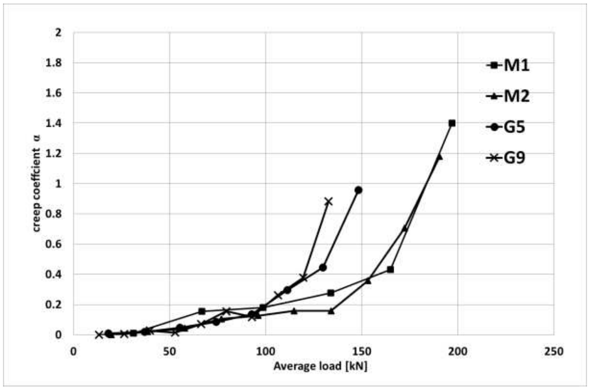

Figure 12. Creep rate in function of the average load

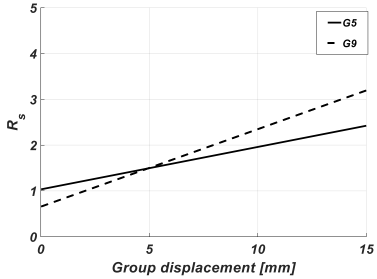

Figure 13. Rs as a function of the group settlement

4 FINITE ELEMENT ANALYSIS

4.1 Introduction

The Finite Element software Plaxis 3D is used in this paper. Large dimensions (20 m x 20 m x 20 m) are considered in the model and the mesh comprises 10-node triangle elements. For a better calculation of large stress concentrations and large deformations, a refined mesh zone around the micropile-soil interface was adopted. Vertical and horizontal fixities were applied to the base, while horizontal fixity was applied to the left and right boundaries. A rigid interface is considered between the micropiles and the soil.

4.2 Constitutive soil and pile model

In this study, the Hardening Soil model with small-strain-stiffness (HSsmall) is used. The required soil parameters are: E_{50}^{ref}, the secant stiffness in standard drained test, E_{oed}^{ref}, the tangent stiffness for primary oedometric loading, E_{ur}^{ref}, the unloading/reloading stiffness, m, the power of stress level dependency of stiffness; c'_{ref}, the cohesion according to the Mohr-Coulomb failure, φ', the angle of internal friction to the Mohr-Coulomb failure, Ψ, the dilatancy angle; $\gamma_{0.7}$, the shear strain at which the shear modulus is equal to 0.72 G_0^{ref}; G_0^{ref}, the shear modulus at very small strain; γ_h, the soil unit weight above phreatic level. Initial soil stresses are generated automatically based on the HS model. All calculations are performed using drained analysis. The micropile is modelled with volume elements and considered as non-porous with a linear-elastic material model.

4.3 Model calibration

Before modelling the micropile groups, it is important to calibrate the model for a single micropile. Soil strength parameters (φ' and c'_{ref}) are first estimated from empirical CPT correlations available in the national Belgian Appendix of Eurocode 7 and in literature (Robertson et al., 1977). For the dilatancy angle, ψ, zero value was considered for φ'-values less than 30°. Otherwise, an order of magnitude of ψ=φ'-30 was assumed. φ' and ψ are then fixed when failure in simulation corresponds to the experiments. Considering the power of stress level dependency of stiffness, m, values of 0.5 and 1 were assumed for sandy and clayey soils, respectively. For silts, an intermediate value is selected Stiffness parameters are more difficult to define. As recommended by Schanz et al. (1999) and in Plaxis manuals for sandy and silty soils, $E_{oed}^{ref}$is usually taken equal to E_{50}^{ref} while E_{ur}^{ref} is typically about 2 to 3 times E_{50}^{ref}. E_{50}^{ref} was initially estimated using Robertson et al, (1977). As a next step, E_{50}^{ref} is progressively adapted until a good match between the measured and simulated load-settlement curve was obtained. Small strain parameters ($\gamma_{0.7}$, G_0^{ref}) are considered according to the empirical relationships of Benz and Vermeer (2009). The calibrated pile and soil parameters are listed in Tables 1 and 2. As the displacement pile was 'wished into place' and no installation effects were considered, the resulting soil strength parameters are slightly higher than for normal conditions. Experience from earlier back calculations show that this is mostly the case to get a good fit.

Table 1. Mechanical pile parameters

Parameters	**loam**	**sandy clay**	**Brusselian sand**
$\gamma_h [kN/m^3]$	17	17	18
E_{50}^{ref} $[MPa]$	30	20	60
$E_{oed}^{ref} [MPa]$	30	20	50
$E_{ur}^{ref} [MPa]$	70	40	170
m [/]	0.7	0.7	0.5
$c'_{ref} [kPa]$	1	5	0
$\varphi' [°]$	33	29	37
$\psi [°]$	3	0	7
$\gamma_{0.7}$ [/]	0.001	0.001	0.001
$G_0^{ref} [MPa]$	90	80	200

Table 2. Mechanical micropile parameters.

Parameter	**Micropile**
$\gamma_h [kN/m^3]$	24
E $[GPa]$	40
ν [/]	0.15o

4.4 Simulations vs. measurements

Figure 14 shows the comparison between finite element simulations and experiments. First a good matching was obtained for single piles in loading and unloading phases. This ensures the good calibration of the model. The same model was then extended to predict the behaviour of the groups. A good agreement was also obtained with G5. The high stiffness of G9 during the first loading stages is not present in simulation which implies the presence of an eventual parasite phenomena during the test setup (eccentricity of the load, temperature effect of measurement cells…). Nevertheless, the tendency of both measurement and simulations is very clear in terms of group effect on the settlement. Figure 15 shows the evolution of Rs in function of the group settlement obtained from FE simulations.

5 CONCLUSIONS

A real-scale test campaign on well-instrumented single micropiles and micropile groups has been set up.

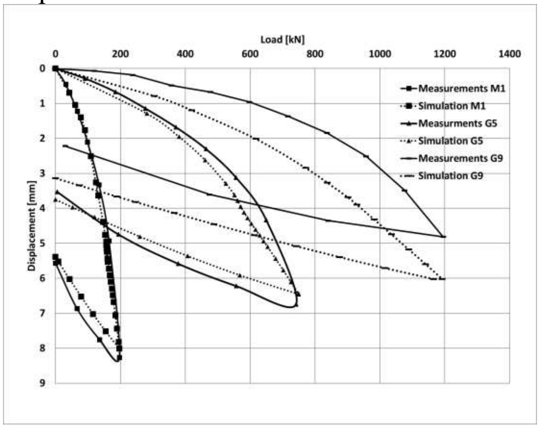

Figure 14. FE simulations versus experiments

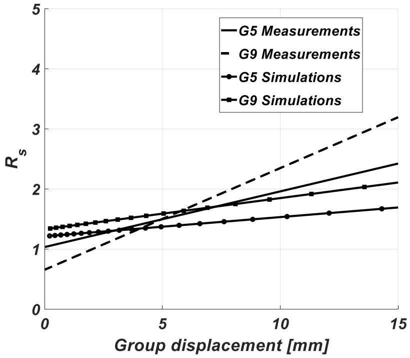

Figure 15. Rs in function of group displacement: simulations versus experiments

The group effect in term of settlement was put in evidence through the measurements. The group settlement ratio Rs is generally greater than 1 especially for large displacements. Rs depends also on the group configuration (Rs for the group G9 is higher than that for G5). This paper pointed out the importance of the soil nonlinearity since Rs increases with the group displacement. A calibrated 3D finite element model was fitted to the measurement. Good agreement was observed for the behaviour of the micropile groups and the dependency of Rs to the group displacement is confirmed.

6 ACKNOWLEDGEMENTS

Special thanks got to the Federal Public Service Economy and the Belgian Bureau for Standardisation (NBN) for their financial support and also to Ischebeck and Denys companies for their support in terms of materials and micropile installation.

7 REFERENCES

Van Alboom, Whenham V. 2003 Soil investigation campaign at Limelette (Belgium): *Proc Symp on screw piles in sand – design & recent developments*, Brussels

Benz, T., Vermeer, P. A., 2009. A small strain overlay model. J. Num. Ana Meth in Geomechanics, **33**, 25-44.

Fleming, W., G., K. 1992. A new method for single pile settlement for prediction and analysis, *Géotechnique*, **42(3)**, 411–425.

Fellenius, B.H. 2001. From strain measurement to load in an instrumented pile, *Geo. News*.

ISSMFE. 1985. Subcommittee on Field and Laboratory Testing, Axial Pile Loading Test, Suggested Method. *ASTM Journal*. 79-90.

Juran, I., Bruce, D.A., Dimillio, A., Benslimane, A. 1999. Micropiles: The state of practice. Part II: Design of single micropiles and groups and networks of micropiles. *Journal of Ground Improvement,* **3**, 89-11

McCabe, B. A., and Lehane, B. M. 2006. Prediction of pile group response using a simplified non-linear finite element model." *Proc., 6th Euro Conf. on Nume Meth in Geotechnical Engineering*,Taylor & Francis, 589–594.

Mylonakis, G., Gazetas, G. 1998. Settlement and additional internal forces of grouped piles in layered soil. *Geotechnique* **48(1)**, 55-72.

Poulos, H.G. and E.H. Davis.1980. *Pile Found. Analysis and Design*. J Wiley and Sons, NY.

Randolph, M. F., Wroth, C. P. 1978. Analysis of deformation of vertically loaded piles. *J. Gotech. Engrg. Div* **104**, 1465–1488.

Robertson, P. K., Lunne, T., Powell, J. J. M.1977. *Cone penetration testing in geotechnical practice.* New York.